

11-9-2018

Origin of localization in Ti-doped Si

Yi Zhang

Louisiana State University

R. Nelson

Rheinisch-Westfälische Technische Hochschule Aachen

K. M. Tam

Louisiana State University

W. Ku

Shanghai Jiao Tong University

U. Yu

Gwangju Institute of Science and Technology

See next page for additional authors

Follow this and additional works at: https://digitalcommons.lsu.edu/physics_astronomy_pubs

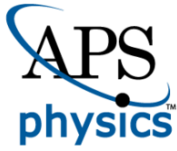
Recommended Citation

Zhang, Y., Nelson, R., Tam, K., Ku, W., Yu, U., Vidhyadhiraja, N., Terletska, H., Moreno, J., Jarrell, M., & Berlijn, T. (2018). Origin of localization in Ti-doped Si. *Physical Review B*, 98 (17) <https://doi.org/10.1103/PhysRevB.98.174204>

This Article is brought to you for free and open access by the Department of Physics & Astronomy at LSU Digital Commons. It has been accepted for inclusion in Faculty Publications by an authorized administrator of LSU Digital Commons. For more information, please contact ir@lsu.edu.

Authors

Yi Zhang, R. Nelson, K. M. Tam, W. Ku, U. Yu, N. S. Vidhyadhiraja, H. Terletska, J. Moreno, M. Jarrell, and T. Berlijn



CHORUS

This is the accepted manuscript made available via CHORUS. The article has been published as:

Origin of localization in Ti-doped Si

Yi Zhang, R. Nelson, K.-M. Tam, W. Ku, U. Yu, N. S. Vidhyadhiraja, H. Terletska, J. Moreno, M. Jarrell, and T. Berlijn

Phys. Rev. B **98**, 174204 — Published 9 November 2018

DOI: [10.1103/PhysRevB.98.174204](https://doi.org/10.1103/PhysRevB.98.174204)

Origin of Localization in Ti doped Si

Yi Zhang,^{1,2,*} R. Nelson,³ K.-M. Tam,^{1,2} W. Ku,⁴ U. Yu,⁵ N. S. Vidhyadhiraja,⁶ H. Terletska,⁷ J. Moreno,^{1,2} M. Jarrell,^{1,2,†} and T. Berlijn^{8,9,‡}

¹Department of Physics & Astronomy, Louisiana State University, Baton Rouge, Louisiana 70803, USA

²Center for Computation & Technology, Louisiana State University, Baton Rouge, Louisiana 70803, USA

³Institute of Inorganic Chemistry, RWTH Aachen University, Landoltweg 1, 52056 Aachen, Germany

⁴Department of Physics and Astronomy, Shanghai Jiao Tong University, Shanghai 200240, China

⁵Department of Physics and Photon Science, GIST, Gwangju 61005, South Korea

⁶Theoretical Sciences Unit, Jawaharlal Nehru Centre for Advanced Scientific Research, Bangalore-560064, India

⁷Department of Physics and Astronomy, Middle Tennessee State University, Murfreesboro, TN 37132, USA

⁸Center for Nanophase Materials Sciences, Oak Ridge National Laboratory, Oak Ridge, TN 37831, USA

⁹Computer Science and Mathematics Division, Oak Ridge National Laboratory, Oak Ridge, Tennessee 37831, USA

Intermediate band semiconductors hold the promise to significantly improve the efficiency of solar cells, but only if the intermediate impurity band is metallic. We apply a recently developed first principles method to investigate the origin of electron localization in Ti doped Si, a promising candidate for intermediate band solar cells. We compute the critical Ti concentration and compare it against the available experimental data. Although Anderson localization is often overlooked in the context of intermediate band solar cells, our results show that in Ti doped Si it plays a more important role in the metal insulator transition than Mott localization. To this end we have devised a way to gauge the relative strengths of these two localization mechanisms that can be applied to study localization in doped semiconductors in general. Our findings have important implications for the theory of intermediate band solar cells.

Introduction.—Intermediate-band solar cells (IBSCs) have been proposed as a candidate for the third generation of photovoltaics^{1–3}. Unlike conventional solar cell materials, intermediate-band photovoltaics are doped with deep-level impurities that induce a partially filled intermediate band located between the valence and the conduction band as shown in Fig. 1. This provides an extra channel for the promotion of an electron from the valence to the conduction band by absorbing two low energy photons instead of one photon with energy greater than the band gap. The extra two-photon channel leads to an increase of photocurrent without decreasing the photovoltage, which could greatly enhance the efficiency of solar cells¹.

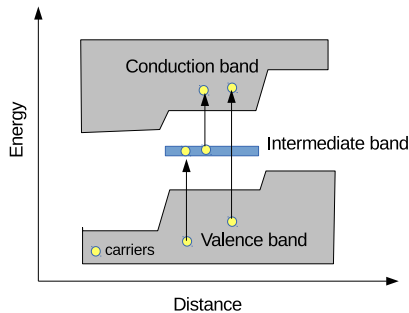


FIG. 1. (color online) Schematic of an intermediate band solar cell (adapted from⁴). Intermediate band states can dramatically improve the efficiency of solar cells by enabling two-photon processes which leads to the increase of photocurrent in a system.

However, the deep-level impurity band also introduces electron-hole pair recombination centers, which normally

lead to the increase of nonradiative Shockley-Reed-Hall (SRH) processes^{5,6} that are detrimental to the efficiency of the solar cell. When an electron or hole is captured by a deep-level impurity state the change in charge around the impurity causes local atomic displacements. According to the microscopic theory of Lang and Henry⁷ these in turn strongly increase the capture cross-section of excited conduction electrons and valence holes into the intermediate band. Based on this theory, Luque *et al.*⁸ argued that if the intermediate band becomes delocalized due to a large density of impurities, the charge of the trapped electron or hole will spread out. This in turn could suppress the atomic displacements and therefore the nonradiative recombinations. This theory has been criticized⁹ but it appears to be consistent with experiments in Ti-doped Si¹⁰ where the carrier lifetime increases with Ti doping. Consequently, a central question is how many impurities are needed to induce an insulator-metal transition in the intermediate band. From a general perspective this question is not only relevant for the efficiency of intermediate band solar cells, but is in fact a fundamental question in condensed matter physics.

In 1977 Anderson and Mott shared one third each of the Nobel prize in physics in part for their study of the localization of electrons in semiconductors. Although they shared this Nobel prize they each had a distinct argument why the electrons become localized^{11,12}. In Mott's model the localization of electrons, or rather the lack thereof, is controlled by the screening of the impurity potentials due to the long-range Coulomb interaction. When an impurity is isolated, it tightly traps the doped carriers. However, when the impurity concentration increases the electrons from one impurity screen the potential of a neighboring impurity thereby causing the electrons to be delo-

calized. We note here that Mott localization should not be confused with Mott-Hubbard localization¹³, in which intra-atomic Coulomb repulsion causes localization by opening a Mott gap. In Anderson's model the localization of electrons occurs purely due to the impurities being disordered. Most studies on IBSCs consider only Mott's criterion for localization^{2-4,14-28}. On the other hand Anderson localization in the context of IBSCs is examined less, either via approximate models⁸ or phenomenological fits²¹ and rarely via first principles calculations²⁹. Unbiased first principles calculations that take into account the material specifics can provide a unique perspective to investigate the relative importance of these two localization mechanisms in IBSCs.

Among the intermediate band semiconductors, Si doped with elements such as Ti has the clear advantage that the host semiconductor is well studied. Moreover, experimental indications for the promise of Ti doped Si are found in electrical resistivity and carrier lifetime measurements^{15,17}. However, to reach an insulator-metal transition in the intermediate band, Ti concentrations beyond the solubility regime are required and non-equilibrium crystal growing techniques need to be applied, which are challenging¹⁰. Therefore independent first principles simulations including the effects of disorder will provide valuable guidance towards achieving high efficiency in Ti doped Si-based IBSCs.

In this letter, we systematically study the metal-insulator transition in Ti doped Si as a function of Ti concentration, by combining two recently developed techniques, the Effective Disorder Hamiltonian Method (EDHM)³⁰ and the Typical Medium Dynamical Cluster Approximation (TMDCA)³¹. We explore the mobility edge separating the delocalized and localized electron states in the intermediate band, and find the critical impurity concentration of the localization transition. Moreover, by theoretically separating the effect of Mott and Anderson localization, we are able to compare these two mechanisms, and find that Anderson dominates over Mott localization in Ti doped Si.

Methods.—First principles simulations take into account the multi-orbital nature of materials and the complex non-local structure of realistic impurity potentials. However, Anderson localization is usually not investigated from first-principles because localized states can be very large and typically need to be simulated with hundreds of thousands of lattice sites³². To overcome the computational expense we have recently developed a method that combines the EDHM and the TMDCA to study Anderson localization from first principles³³. We have already applied this combined method to superconductors³³, dilute magnetic semiconductors³⁴, and here are applying it to the intermediate band semiconductor Ti doped Si. For another recent computational approach to study Anderson localization from first principles we refer to Ref. 29.

The EDHM³⁰ is a Wannier function^{35,36} based method which allows to derive accurate low-energy tight-binding

models of disordered materials from DFT calculations as has been demonstrated in numerous case studies^{30,37-40}. Specifically, models of both undoped Si and a supercell with a single Ti impurity are derived in the Wannier basis functions of Si-*s*, Si-*p* and Ti-*d*, and the impurity potential is captured by the difference of these two models. Experimental measurements and theoretical calculations^{15,19} have shown that the Ti dopants are mostly interstitial impurities rather than (Si,Ti) substitutions and hence we focus here on Ti interstitials. To capture the experimental band-gap of Si we apply the LDA+U approximation, which we found to compare accurately with the modified Becke-Johnson potential^{41,42}. In this study we used three different sizes of supercells: TiSi₈, TiSi₆₄ and TiSi₂₁₆ which lead to three different impurity potentials.

Next we use the low-energy tight-binding model of pure Si and the Ti impurity potentials obtained from the EDHM as input for the TMDCA. The TMDCA is a cluster extension of the typical medium theory (TMT)⁴³, which in turn is a modification of the coherent potential approximation (CPA)⁴⁴, where a geometric average of the local density of states (DOS): $(\text{DOS}_1 \cdot \text{DOS}_2 \cdot \dots \cdot \text{DOS}_N)^{1/N}$ is carried out in the impurity solver instead of the usual arithmetic average: $(\text{DOS}_1 + \text{DOS}_2 + \dots + \text{DOS}_N)/N$. Here DOS_i is the DOS at a particular site in a particular disorder configuration and N is the total number of sites. The resulting geometrically averaged DOS or typical density of states (TDOS) captures the physics of localization^{43,45}. TDOS is finite in the delocalized phase and vanishes at the localized phase and so serves as an order parameter for the transition. Therefore, by comparing DOS and TDOS in the same plot, we are able to determine which states are localized and which are metallic. TMDCA overcomes the restrictions of the TMT and accurately predicts the critical disorder strength of the single-band Anderson model with uniform disorder³¹. In order to deal with more complicated realistic systems, the TMDCA is extended to systems with off-diagonal disorder⁴⁶ and to multi-band systems³³. For both extensions the TMDCA has been found to accurately reproduce the localization phase diagrams obtained with well established theoretical methods such as the transfer matrix method and the kernel polynomial method^{33,46}.

Results.—First, we derive the critical concentration for the metal insulator transition in Ti doped Si by calculating DOS and TDOS for various Ti concentrations, x . We have checked convergence against various computational parameters⁴¹. Fig. 2 displays the concentration x evolution of the DOS and TDOS. The band roughly above 1.25 eV corresponds to the conduction band and the one below 0 eV is the valence band. The partially filled intermediate band is centered within [0.25,0.35] eV below the conduction band in agreement with experimental observations^{15-17,47,48} that range within [0.21,0.36] eV. Let us focus first on the results derived from the TiSi₂₁₆ supercell. For the relatively large Ti concentrations, $x=1\%$,

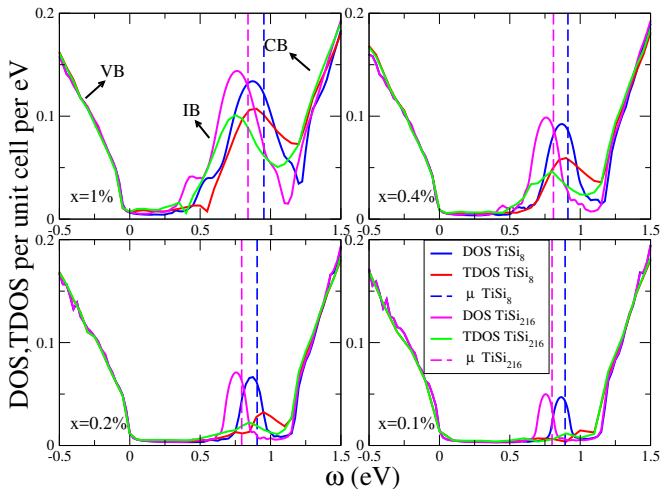


FIG. 2. (color online) Density of States (DOS) and Typical Density of States (TDOS) of Ti doped Si for various Ti concentrations: $x = 1\%$, 0.4% , 0.2% , 0.1% . Two sets of results are presented based on the impurity potentials from supercell calculations with two difference sizes: TiSi_8 and TiSi_{216} . VB, CB, and IB correspond to the valence, conduction and intermediate band, respectively. The chemical potentials are indicated by dashed lines.

the TDOS of the impurity band is finite indicating that its states are delocalized, i.e., metallic. As the Ti concentration x decreases, the TDOS of the intermediate band gradually decreases and starts to vanish at concentrations between $x=0.2\%$ and $x=0.1\%$ signaling the localization transition. These values correspond to a critical Ti concentration between $1.0 \times 10^{20} \text{ cm}^{-3}$ and $5.0 \times 10^{19} \text{ cm}^{-3}$, which is consistent with some of the available experimental results^{18,49}, but not others⁵⁰. We have checked that neither lattice relaxation, nor spin-polarization effects change this conclusion significantly⁴¹. Both theoretical calculations and experiments have shown that such high concentrations of Ti in Si are thermodynamically unstable^{10,19}. Hence non-equilibrium growth techniques have been employed to increase doping¹⁰. Drawbacks of such preparation methods are inhomogeneous distributions of dopants and damage to the crystal structure. Still the effect of these nonidealities is not strong enough to counteract the experimentally observed lifetime recovery¹⁰. Furthermore, a recent study²⁸ shows that the cellular breakdown in Ti doped Si can be suppressed for Ti concentrations as high as 6%. Despite the progress, hyperdoping Si with Ti remains challenging and conflicting results have been reported about the metal insulator transition in Ti doped Si^{18,49,50}. Therefore our first principles derivation of the critical concentration is a valuable benchmark. However, the theoretical derivation of the critical concentration by itself does not answer the question what causes the metal-insulator transition in Ti doped Si: is it Mott localization or Anderson localization?

To investigate the relative importance of Mott's and

Anderson's localization mechanisms we will now explore the effects of screening in our simulation. In Mott's original picture¹², the electronic impurity states are assumed to be localized, discrete, and bound to the impurity. As the number of impurities increases, however, the binding potential of one impurity undergoes Thomas-Fermi screening by the long-range Coulomb potentials of the electrons on the surrounding impurities. The Mott transition from insulator to metal occurs when this screening reduces the strength of the impurity potential below a critical value, squeezing the impurity state into the continuum and forming a metal. Unlike the effects of Mott-Hubbard localization caused by intra-atomic Coulomb repulsion, Mott's model based on Thomas-Fermi screening can be captured accurately within DFT. In doped semiconductors Mott and Anderson localization are entangled⁵¹ and it is usually quite challenging to distinguish them. However, it turns out that within our EDHM+TMDCA method the separation of Mott's and Anderson's mechanisms is natural.

In Mott's picture of localization, the states are pushed into the continuum due to the screening of the potential, while in Anderson localization, the states are localized due to disorder. Therefore, by tuning the strength of screening and disorder separately, we are able to distinguish the effect of Mott and Anderson localizations. In our method, the strength of disorder is tuned by the concentration of impurities in the TMDCA calculation, while the screening effect as captured by the EDHM is frozen in the impurity potential. By changing the size of the supercell used for the EDHM when deriving the impurity potential, we have a separate knob to tune the strength of the screening effect. Based on this, we derive the impurity potential from three different supercell sizes: TiSi_8 , TiSi_{64} and TiSi_{216} . Given that the Ti concentration in the TiSi_8 supercell is 27 times larger than in the TiSi_{216} supercell one would expect based on Mott's mechanism a strong reduction of the impurity potential and therefore a decrease in the localization. However, as shown in Fig. 2 we distinguish no significant effect on the localization from the TMDCA based on these two impurity potentials. For each of the four disorder concentrations we see only minor changes in the DOS and TDOS for the TiSi_8 and TiSi_{216} derived impurity potentials. The relative difference between the DOS and TDOS is much more sensitive to changes in disorder than to the changes in the screening. The DOS and TDOS vary even much less when the impurity potentials from TiSi_{64} and TiSi_{216} are compared⁴¹. More importantly, the critical impurity concentration for all three investigated screening strengths lies between $x=0.2\%$ and $x=0.1\%$. This indicates that the screening induced Mott localization plays a marginal role here compared to Anderson localization, despite the fact that most studies on IBSCs focus on Mott's criterion only. The above described approach of gauging the relative strengths of the Mott and Anderson localization methods is not just limited to Ti doped Si, but can be applied to doped semiconductors in general.

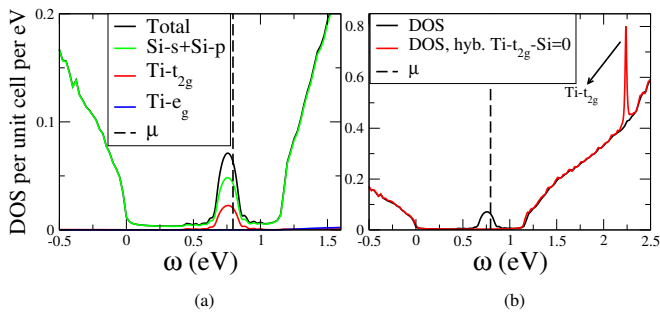


FIG. 3. (color online) Density of States (DOS) of Ti doped Si for Ti concentration $x=0.2\%$ based on the impurity potential derived from the TiSi_{216} supercell. (a) Orbital resolved contributions. (b) DOS when hybridization between $\text{Ti-}t_{2g}$ and $\text{Si-}s$, $\text{Si-}p$ is removed. The dashed line indicates the chemical potential.

To understand the weak effect of Mott's screening on Ti doped Si we take a closer look at the electronic structure of the impurity band complex. Fig. 3(a) shows the DOS of Si with 0.2% of Ti impurities, now resolving the partial contributions from $\text{Ti-}t_{2g}$, $\text{Ti-}e_g$ and $\text{Si-}s/\text{Si-}p$. As we can see the intermediate band complex consists of a strong mixture of $\text{Ti-}t_{2g}$, $\text{Si-}s$ and $\text{Si-}p$. Clearly the hybridization of the $\text{Ti-}t_{2g}$ orbitals with $\text{Si-}s/\text{Si-}p$ plays an important role in the formation of the impurity band. To better illustrate this we plot in Fig. 3(b) the total DOS for a calculation in which we switch off the hybridization of $\text{Ti-}t_{2g}$ with $\text{Si-}s$ and $\text{Si-}p$ in our effective tight-binding model. Fig. 3(b) shows that in that case the impurity band vanishes from the gap and ends up about 1 eV above the bottom of the conduction band. In other words the hybridization of $\text{Ti-}t_{2g}$ with $\text{Si-}s$ and $\text{Si-}p$ is what creates the impurity band and this explains why the effects of screening are so weak in Ti doped Si. The main effect of the Ti impurity is coming from the overlaps of the $\text{Ti-}t_{2g}$ wave functions with those of the $\text{Si-}s$ and $\text{Si-}p$ wave functions and those are affected only weakly by screening at most. For example, the largest element in our first principles derived impurity potential is a hopping element between $\text{Ti-}t_{2g}$ and a nearest neighboring $\text{Si-}p$ orbital. Its value of 1.4 eV differs only by 1 meV when its extracted from the TiSi_8 supercell instead of the TiSi_{216} supercell. Based on this microscopic insight we expect that our conclusion on the weakness of screening effects in Ti doped Si can be generalized to other IB semiconductors. In particular, in transition metal doped intermediate band semiconductors such as Co doped Si^{23} , V doped In_2S_3 ⁵², Ti doped GaAs^{53} and Cr doped AlP^{54} , we can expect a strong hopping disorder, given that the transition metal d impurity orbitals are highly distinct from the s and p host orbitals. On the other hand, in S doped Si the impurity and host atoms are chemically close to each other because S and Si are in the same row and only two columns apart in the periodic table. Therefore the impurity band in this case is expected to be less controlled by hopping to impurity

sites and hence more susceptible to screening effects, explaining why long range Coulomb effects in S doped Si may play a more important role²¹.

Our finding that in Ti doped Si Anderson localization dominates over Mott localization has important consequences for the theory of intermediate band solar cells in this system and others like it, given that the nature of these two localization mechanisms is fundamentally different. First of all, the Mott transition is believed to be first order¹², whereas the Anderson transition is a second order phase transition⁵⁵. Therefore, one expects a less abrupt lifetime recovery as a function of Ti doping for Anderson localization than for the Mott's mechanism. Concurrently, there should be a smooth drop in the resistivity across the critical concentration rather than an abrupt one, which provides a signature to be looked for in future experiments. Furthermore, a Mott localized state is trapped by a single impurity whereas the Anderson localized state is typically trapped by a cluster of impurities that has a large extent in space²⁹. This means that the charge in an Anderson localized state will be more spread out and less likely to cause non-radiative recombinations than in a Mott localized state. Finally, the Anderson transition is a quantum phase transition only defined at zero temperature⁵⁵, whereas the relevant temperature for IBSCs is room temperature. However, it has been shown that effects of the Anderson localization, such as variable range hopping, extend to room temperature and beyond⁵⁶⁻⁵⁸. Moreover, even if an electron hops between Anderson localized states via interaction with phonons⁵⁹, an important question is how fast it will do so. If the time scale is larger or comparable to the carrier lifetime then the Anderson localization should still strongly affect the non-radiative recombination rate. Given that both variable range hopping and non-radiative recombinations are controlled by phonons, it is conceivable that their time scales be comparable. The above implications for the theory of IBSCs highlight the richness of the physics of Anderson localization and that of disordered materials in general.

In summary, by combining two recently developed theoretical techniques, the EDHM and the TMDCA, we investigate from first principles the metal-insulator transition in the promising intermediate-band photovoltaic material Ti doped Si. We systematically study the localization in the impurity band and find that the impurity band electrons delocalize for a Ti concentration between $x=0.1\%$ and $x=0.2\%$. These results provide a valuable benchmark given the conflicting experimental reports on the critical Ti concentration in Ti doped Si. Our calculation can be applied to other systems with intermediate bands providing guidance to make highly efficient IB solar cells. Moreover, our approach provides a systematic way to study the nature of the localization transition by separating the effects of Mott and Anderson localization. Our results show that in Ti doped Si, Anderson localization dominates over Mott localization, despite that most studies on intermediate band solar cells consider Mott's

criterion for localization only. The reason for the weakness of Mott localization here is that the impurity band is induced by the hopping between $Ti-t_{2g}$ and $Si-s/Si-p$ orbitals, an effect that can not be diminished by screening. Given the fundamental differences between Mott and Anderson localization our finding has important implications for the theory of intermediate band solar cells.

This letter is based upon work supported by the U.S. Department of Energy, Office of Science, Office of Basic Energy Sciences under Award Number DE-SC0017861. Work by TB was performed at the Center

for Nanophase Materials Sciences, a DOE Office of Science user facility. This manuscript has been authored by UT-Battelle, LLC under Contract No. DE-AC05-00OR22725 with the U.S. Department of Energy. This work used the high performance computational resources provided by the Louisiana Optical Network Initiative (<http://www.loni.org>), and HPC@LSU computing. Furthermore, this research used resources of the National Energy Research Scientific Computing Center, a DOE Office of Science User Facility supported by the Office of Science of the U.S. DOE under Contract No. DE-AC02-05CH11231.

* zhangyiphys@gmail.com

† jarrellphysics@gmail.com

‡ tberlijn@gmail.com

¹ A. Luque and A. Martí, *Phys. Rev. Lett.* **78**, 5014 (1997).

² A. Luque and A. Martí, *Adv. Mater.* **22**, 160 (2010).

³ Y. Okada, N. J. Ekins-Daukes, T. Kita, R. Tamaki, M. Yoshida, A. Pusch, O. Hess, C. C. Phillips, D. J. Farrell, K. Yoshida, N. Ahsan, Y. Shoji, T. Sogabe, and J.-F. Guillemoles, *Appl. Phys. Rev.* **2**, 021302 (2015).

⁴ A. Luque, A. Martí, and C. Stanley, *Nat. Photonics* **6**, 146 (2012).

⁵ W. Shockley and W. T. Read, *Phys. Rev.* **87**, 835 (1952).

⁶ R. N. Hall, *Phys. Rev.* **87**, 387 (1952).

⁷ D. V. Lang and C. H. Henry, *Phys. Rev. Lett.* **35**, 1525 (1975).

⁸ A. Luque, A. Martí, E. Antolín, and C. Tablero, *Physica B* **382**, 320 (2006).

⁹ J. J. Krich, B. I. Halperin, and A. Aspuru-Guzik, *J. Appl. Phys.* **112**, 013707 (2012), <http://dx.doi.org/10.1063/1.4732085>.

¹⁰ E. Antolín, A. Martí, J. Olea, D. Pastor, G. González-Díaz, I. Mártil, and A. Luque, *Appl. Phys. Lett.* **94**, 042115 (2009).

¹¹ P. W. Anderson, *Phys. Rev.* **109**, 1492 (1958).

¹² N. F. Mott, *Rev. Mod. Phys.* **40**, 677 (1968).

¹³ M. Imada, A. Fujimori, and Y. Tokura, *Rev. Mod. Phys.* **70**, 1039 (1998).

¹⁴ A. Martí, D. F. Marrón, and A. Luque, *Journal of Applied Physics* **103**, 073706 (2008).

¹⁵ J. Olea, M. Toledano-Luque, D. Pastor, G. González-Díaz, and I. Mártil, *J. Appl. Phys.* **104**, 016105 (2008).

¹⁶ J. Olea, G. González-Díaz, D. Pastor, and I. Mártil, *Journal of Physics D: Applied Physics* **42**, 085110 (2009).

¹⁷ J. Olea, M. Toledano-Luque, D. Pastor, E. San-Andrés, I. Mártil, and G. González-Díaz, *J. Appl. Phys.* **107**, 103524 (2010).

¹⁸ J. Olea, D. Pastor, E. García-Hemme, R. García-Hernansanz, Á. del Prado, I. Mártil, and G. González-Díaz, *Thin Solid Films* **520**, 6614 (2012).

¹⁹ K. Sánchez, I. Aguilera, P. Palacios, and P. Wahnón, *Phys. Rev. B* **79**, 165203 (2009).

²⁰ G. González-Díaz, J. Olea, I. Mártil, D. Pastor, A. Martí, E. Antolín, and A. Luque, *Solar Energy Materials and Solar Cells* **93**, 1668 (2009).

²¹ M. T. Winkler, D. Recht, M.-J. Sher, A. J. Said, E. Mazur, and M. J. Aziz, *Phys. Rev. Lett.* **106**, 178701 (2011).

²² Y. Zhou, F. Liu, M. Zhu, X. Song, and P. Zhang, *Applied Physics Letters* **102**, 222106 (2013).

²³ Y. Zhou, F. Liu, and X. Song, *Journal of Applied Physics* **113**, 103702 (2013), <https://doi.org/10.1063/1.4794818>.

²⁴ D. Pastor, J. Olea, A. del Prado, E. García-Hemme, R. García-Hernansanz, I. Mártil, and G. González-Díaz, *Journal of Physics D: Applied Physics* **46**, 135108 (2013).

²⁵ S. Hu, P. Han, P. Liang, Y. Xing, and S. Lou, *Materials Science in Semiconductor Processing* **17**, 134 (2014).

²⁶ X. Dong, X. Song, Y. Wang, and J. Wang, *Applied Physics Express* **8**, 081302 (2015).

²⁷ M. A. Flores and E. Menéndez-Proupin, *Journal of Physics: Conference Series* **720**, 012033 (2016).

²⁸ F. Liu, S. Prucnal, R. Hbner, Y. Yuan, W. Skorupa, M. Helm, and S. Zhou, *Journal of Physics D: Applied Physics* **49**, 245104 (2016).

²⁹ E. G. Carnio, N. D. M. Hine, and R. A. Römer, *ArXiv e-prints* (2017), [arXiv:1710.01742](https://arxiv.org/abs/1710.01742).

³⁰ T. Berlijn, D. Volja, and W. Ku, *Phys. Rev. Lett.* **106**, 077005 (2011).

³¹ C. E. Ekuma, H. Terletska, K.-M. Tam, Z.-Y. Meng, J. Moreno, and M. Jarrell, *Phys. Rev. B* **89**, 081107 (2014).

³² L. J. Vasquez, A. Rodriguez, and R. A. Römer, *Phys. Rev. B* **78**, 195106 (2008).

³³ Y. Zhang, H. Terletska, C. Moore, C. Ekuma, K.-M. Tam, T. Berlijn, W. Ku, J. Moreno, and M. Jarrell, *Phys. Rev. B* **92**, 205111 (2015).

³⁴ Y. Zhang, R. Nelson, E. Siddiqui, K.-M. Tam, U. Yu, T. Berlijn, W. Ku, N. S. Vidhyadhiraja, J. Moreno, and M. Jarrell, *Phys. Rev. B* **94**, 224208 (2016).

³⁵ N. Marzari and D. Vanderbilt, *Phys. Rev. B* **56**, 12847 (1997).

³⁶ W. Ku, H. Rosner, W. E. Pickett, and R. T. Scalettar, *Phys. Rev. Lett.* **89**, 167204 (2002).

³⁷ T. Berlijn, C.-H. Lin, W. Garber, and W. Ku, *Phys. Rev. Lett.* **108**, 207003 (2012).

³⁸ T. Berlijn, P. J. Hirschfeld, and W. Ku, *Phys. Rev. Lett.* **109**, 147003 (2012).

³⁹ L. Wang, T. Berlijn, Y. Wang, C.-H. Lin, P. J. Hirschfeld, and W. Ku, *Phys. Rev. Lett.* **110**, 037001 (2013).

⁴⁰ T. Berlijn, H.-P. Cheng, P. J. Hirschfeld, and W. Ku, *Phys. Rev. B* **89**, 020501 (2014).

⁴¹ Technical details are provided in the Supplementary Information, which includes Refs.^{60–64}.

⁴² F. Tran and P. Blaha, *Phys. Rev. Lett.* **102**, 226401 (2009).

⁴³ V. Dobrosavljević, A. A. Pastor, and B. K. Nikolić, *Euro-*

- phys. Lett. **62**, 76 (2003).
- ⁴⁴ P. Soven, Phys. Rev. **156**, 809 (1967).
- ⁴⁵ A. Weiße, G. Wellein, A. Alvermann, and H. Fehske, Rev. Mod. Phys. **78**, 275 (2006).
- ⁴⁶ H. Terletska, C. E. Ekuma, C. Moore, K.-M. Tam, J. Moreno, and M. Jarrell, Phys. Rev. B **90**, 094208 (2014).
- ⁴⁷ D. Mathiot and S. Hocine, Journal of Applied Physics **66**, 5862 (1989), <https://doi.org/10.1063/1.343608>.
- ⁴⁸ J.-W. Chen, A. Milnes, and A. Rohatgi, Solid-State Electronics **22**, 801 (1979).
- ⁴⁹ J. Olea, E. Lpez, E. Antoln, A. Mart, A. Luque, E. Garca-Hemme, D. Pastor, R. Garca-Hernansanz, A. del Prado, and G. Gonzlez-Daz, Journal of Physics D: Applied Physics **49**, 055103 (2016).
- ⁵⁰ F. Liu, M. Wang, Y. Berencén, S. Prucnal, M. Engler, R. Hübner, Y. Yuan, R. Heller, R. Böttger, L. Rebohle, W. Skorupa, M. Helm, and S. Zhou, Sci. Rep. **8**, 4164 (2018).
- ⁵¹ T. F. Rosenbaum, R. F. Milligan, M. A. Paalanen, G. A. Thomas, R. N. Bhatt, and W. Lin, Phys. Rev. B **27**, 7509 (1983).
- ⁵² R. Lucena, I. Aguilera, P. Palacios, P. Wahnón, and J. C. Conesa, Chemistry of Materials **20**, 5125 (2008).
- ⁵³ C. D. Brandt, A. M. Hennel, T. Bryskiewicz, K. Y. Ko, L. M. Pawlosicz, and H. C. Gatos, Journal of Applied Physics **65**, 3459 (1989).
- ⁵⁴ P. Olsson, C. Domain, and J.-F. Guillemoles, Phys. Rev. Lett. **102**, 227204 (2009).
- ⁵⁵ E. Abrahams, *50 Years of Anderson Localization* (World Scientific, 2010).
- ⁵⁶ K. L. Chopra and S. K. Bahl, Phys. Rev. B **1**, 2545 (1970).
- ⁵⁷ C. W. Bates and C. Zhang, AIP Advances **3**, 102111 (2013).
- ⁵⁸ J. J. van Hapert, *Hopping Conduction and Chemical Structure: a study on Silicon Suboxides*, Ph.D. thesis, Utrecht University (1973).
- ⁵⁹ V. Ambegaokar, B. I. Halperin, and J. S. Langer, Phys. Rev. B **4**, 2612 (1971).
- ⁶⁰ K. Schwarz, P. Blaha, and G. Madsen, Computer Physics Communications **147**, 71 (2002), proceedings of the Europhysics Conference on Computational Physics Computational Modeling and Simulation of Complex Systems.
- ⁶¹ J. P. Perdew, K. Burke, and M. Ernzerhof, Phys. Rev. Lett. **77**, 3865 (1996).
- ⁶² D. Töbrens, N. Stüßer, K. Knorr, H. Mayer, and G. Lampert, in *European Powder Diffraction EPDIC 7*, Materials Science Forum, Vol. 378 (Trans Tech Publications, 2001) pp. 288–293.
- ⁶³ M. Jarrell and H. R. Krishnamurthy, Phys. Rev. B **63**, 125102 (2001).
- ⁶⁴ V. I. Anisimov, I. V. Solovyev, M. A. Korotin, M. T. Czyżyk, and G. A. Sawatzky, Phys. Rev. B **48**, 16929 (1993).